Published in final edited form as:
Urology. 2011 July ; 78(1): 225–231. doi:10.1016/j.urology.2011.02.057.

Dynamic Real-time Microscopy of the Urinary Tract Using Confocal Laser Endomicroscopy

Katherine Wu, **Jen-Jane Liu**, **Winifred Adams**, **Geoffrey A. Sonn**, **Kathleen E. Mach**, **Ying Pan**, **Andrew H. Beck**, **Kristin C. Jensen**, and **Joseph C. Liao**
Department of Urology and Department of Pathology, Stanford Cancer Center and the Bio-X Program, Stanford University School of Medicine, Stanford, California; and the Veterans Affairs Palo Alto Health Care System, Palo Alto, California

Abstract

OBJECTIVES—To develop the diagnostic criteria for benign and neoplastic conditions of the urinary tract using probe-based confocal laser endomicroscopy (pCLE), a new technology for dynamic, in vivo imaging with micron-scale resolution. The suggested diagnostic criteria will formulate a guide for pCLE image interpretation in urology.

METHODS—Patients scheduled for transurethral resection of bladder tumor (TURBT) or nephrectomy were recruited. After white-light cystoscopy (WLC), fluorescein was administered as contrast. Different areas of the urinary tract were imaged with pCLE via direct contact between the confocal probe and the area of interest. Confocal images were subsequently compared with standard hematoxylin and eosin analysis.

RESULTS—pCLE images were collected from 66 participants, including 2 patients who underwent nephrectomy. We identified key features associated with different anatomic landmarks of the urinary tract, including the kidney, ureter, bladder, prostate, and urethra. In vivo pCLE of the bladder demonstrated distinct differences between normal mucosa and neoplastic tissue. Using *mosaicing*, a post hoc image-processing algorithm, individual image frames were juxtaposed to form wideangle views to better evaluate tissue microarchitecture.

CONCLUSIONS—In contrast to standard pathologic analysis of fixed tissue with hematoxylin and eosin, pCLE provides real time microscopy of the urinary tract to enable dynamic interrogation of benign and neoplastic tissues in vivo. The diagnostic criteria developed in this study will facilitate adaptation of pCLE for use in conjunction with WLC to expedite diagnosis of urinary tract pathology, particularly bladder cancer.

White-light cystoscopy (WLC), the standard approach to evaluate the lower urinary tract, has several well-recognized shortcomings, particularly in differentiating nonpapillary urothelial carcinoma from inflammatory lesions and delineation of tumor boundaries.[1] Although histology remains the cornerstone of cancer diagnosis, it is not readily available in real time to guide surgical intervention. Significant interest exists in developing adjunctive imaging technologies to overcome the shortcomings of WLC—particularly to identify

Reprint requests: Joseph C. Liao, M.D., Department of Urology, Stanford University School of Medicine, 300 Pasteur Drive, S-287, Stanford, CA 94305-5118. jliao@stanford.edu.

tumors with clinically aggressive features— thereby improving the quality and yield of transurethral resection and overall clinical outcomes.

Several optical imaging technologies have recently been approved for the urinary tract, including fluorescence cystoscopy (photodynamic diagnosis), narrow band imaging, and optical coherence tomography.[2–7] Probebased confocal laser endomicroscopy (pCLE) is another emerging technology under investigation.[8,9] Based on the established principle of confocal microscopy, pCLE provides in vivo microscopy of living tissues through miniaturized fiberoptic probes inserted through working channels of standard endoscopes, including cystoscopes. In contrast to other imaging technologies, pCLE has micron- scale resolution, thus making it possible to visualize tissue microarchitecture and cellular morphology reminiscent of histology. Currently, pCLE is approved for clinical use in the respiratory and gastrointestinal tracts.[10–14] For Barrett's esophagus, a precancerous entity in which WL diagnosis is also challenging, sensitivity of 88% and specificity of 96% with excellent interobserver agreement have recently been reported with pCLE.[15]

The goal of the current study is to expand upon our initial feasibility study to provide in-depth characterization of the confocal microscopy features of benign and neoplastic regions of the urinary tract. Although building diagnostic criteria for bladder cancer remains the focus, confocal features of urethra, prostate, ureter, and kidney are also investigated. For image analysis, we evaluated a computer algorithm called *mosaicing*, which provides a panoramic view of the microarchitecture.[16–18] The resulting collection of images and suggested diagnostic criteria provide the foundation for a prospective diagnostic accuracy study of pCLE for bladder cancer diagnosis.

MATERIAL AND METHODS

Probe-Based Confocal Laser Endomicroscopy

Confocal microscopy of the urinary tract was performed with the Cellvizio system (Mauna Kea Technologies, Paris, France), and consisted of a fiberoptic imaging probe, a laser scanning unit, and a desktop computer with the image acquisition and processing software. In addition to the previously described 2.6-mm-diameter probe (GastroFlex UHD),8 a 1.4-mm probe (AlveoFlex) was used in this study. The 2.6-mm probe has a resolution of 1 μm and a field of view (FOV) of 240 μm, whereas the 1.4-mm probe has a resolution of 3.5 μm and an FOV of 600 μm. The probes were sterilized after each use with either the System 1 (Steris, Mentor, OH) or the STERRAD 200 (ASP, Irvine, CA) system. Images were collected as video sequences at 12 frames per second through direct contact of the tissue with the probe.

Imaging Protocol

The study was approved by the Stanford University Institutional Review Board and VAPAHCS Research and Development Committee. Consecutive patients scheduled for cystoscopic biopsy or TURBT, in addition to 2 patients who underwent nephrectomy, provided consent. After initial examination with WLC, all patients received fluorescein (Alcon Laboratories, Fort Worth, TX) intravesically and/or intravenously. Fluorescein (MW

= 332.3 g/mL) is approved by Federal Drug Administration for intravenous use for ophthalmologic imaging of blood vessels and has recently been shown to be a safe contrast agent for pCLE in the gastrointestinal tract.19 For intravesical administration, 300–400 mL of 0.1% fluorescein diluted in normal saline was instilled into the bladder via a Foley catheter and left indwelling for 5 minutes. For intravenous administration, 0.5 mL of 10% fluorescein was given immediately before pCLE imaging.

Confocal images were obtained with the 2.6-mm probe inserted through standard 26-Fr resectoscope or with the 1.4-mm probe in standard rigid (21-Fr) or flexible (15-Fr) cystoscopes. WLC videos were recorded simultaneously and selected still images taken. By varying the probe pressure on the surface, different layers of the epithelium of the lower urinary tract were imaged. Kidneys from 2 nephrectomy patients were used for ex vivo confocal imaging of the renal cortex, pelvis, and proximal ureter. Topical fluorescein was applied ex vivo in 1 kidney, while intravenous fluorescein was given before division of the renal hilum in the other. Imaged tissue locations were biopsied or resected and sent for pathologic analysis with hematoxylin and eosin (H&E) staining. Acquired confocal video sequences were edited and analyzed after the procedure and compared with H&E-stained tissue.

Mosaicing Algorithm

The mosaicing algorithm (Mauna Kea Technologies) is an image-processing technique that compiles a series of consecutive images into a single larger composite image that effectively increases the FOV.16,17 It is based on a hierarchical framework that recovers a globally consistent alignment of input frames to compensate for distortions induced by the relative motion of imaged tissue with respect to the probe.[18]

Image Selection Criteria

After real-time confocal video sequences were acquired, videos were processed offline before image characteristics were analyzed. Video clips and still images of interest were extracted from the original sequences. Clips were selected based on clarity of images and probe contact time longer than 2 seconds. Mosaics were created using the algorithm described above. Processed confocal images were reviewed with 2 pathologists (K.C.J., A.H.B.) and compared with corresponding H&E stains. Diagnostic criteria representative of different types of bladder cancer were selected based on reproducibility and correspondence to H&E histology. Imaging characteristics that were easily recognizable and reproducible by the urologist (J.C.L.) were chosen for use as diagnostic criteria. Representative images for the atlas were chosen based on resemblance to corresponding H&E images as well as image quality, taking into account motion and lens artifacts and level of staining.

RESULTS

To compile the imaging atlas, 566 real-time confocal video sequences from 66 study participants (mean age 71 years, range 28–90 years) were analyzed. The mean duration of confocal image acquisition was 15.5 minutes per participant. Average probe dwell time for each area was 11.4 seconds and the average number clips per area was 4.3. There were no

adverse events related to pCLE or fluorescein administration, other than transient fluorescence- stained urine. No differences were noted in histology quality of tissue treated with IV or intravesical fluorescein.

We evaluated *mosaicing*, an image processing technique that juxtaposes overlapping frames into a single composite image, thus expanding the FOV while improving overall image resolution. Figure 1 shows representative mosaics of the umbrella cell layer of normal urothelium (Fig. 1A) and prostatic urethra (Fig. 1B). Compared with individual image frames (figure inset), the composite mosaics expanded the FOV by up to 5-fold (from 0.24 to 1.27 mm). The characteristic polygonal-shaped umbrella cells, visualized in vivo, were reminiscent of the ex vivo images of umbrella cells obtained using more powerful desktop confocal microscopes.[20,21] The glandular structures visualized through the prostatic urethra after IV fluorescein administration are consistent with benign prostatic glands.

Figure 2 shows representative confocal images of the normal anatomic landmarks from the entire urinary tract. Confocal microscopy of the lower urinary tract was acquired in vivo, whereas upper tract images were obtained ex vivo. With either intravesical or intravenous fluores- cein administration, circulating erythrocytes were routinely observed within the rich capillary network of the lamina propria. The results indicate that within 5 minutes of intravesical instillation, fluorescein diffuses across the transitional cell layers into the lamina propria. Normal bladder urothelium was characterized by a polygonal umbrella cell layer, uniform smaller intermediate cell layer, and capillary networks with erythrocytes in the lamina propria (Figs. 1A and 2). Although the limited depth of penetration prohibited imaging beyond the lamina propria through intact urothelium, the fibers of the muscularis propria and the adipocytes of the perivesical fat were imaged in the tumor resection bed in 14 participants. In the penile urethra, the lamina propria is characterized by branching thin dark bands that likely represent small vessels. In this first reported application of pCLE of the upper urinary tract, the renal cortex was characterized by tubular structures consistent with convoluted renal tubules, while renal pelvis and proximal ureter showed urothelial cells and lamina propria similar to bladder urothelium.

Confocal features of low grade urothelial carcinoma were defined by analysis of 64 confocal videos from 22 pathologically confirmed tumors, most of which were papillary by WLC. Figure 3A–F shows the diagnostic confocal features of low grade tumors, including densely packed urothelial cells that are homogenous and monomorphic. Other characteristics include cellular papillary structures and fibrovascular stalks from tumor neoangiogenesis that were not observed in normal or inflamed areas. During real-time imaging, fibrovascular stalks were easily visualized because of the constant flow of erythrocytes.

For high grade urothelial carcinoma, 73 confocal videos from 27 pathologically confirmed tumors were ana- lyzed. With WLC, high-grade tumors were variable in appearance, ranging from papillary, to sessile, to flat. Microscopically, confocal criteria for high grade tumors overlap with those of low grade, including densely packed cells and presence of fibrovascular stalks. Consistently, however, high grade tumors exhibited a far more distorted microarchitecture; these tumors exhibited a pleomorphic population of irregularly shaped cells with loss of cellular cohesiveness, indistinct cell borders, and disorganized vasculature

(Fig. 3G–J). Interestingly, neither the umbrella cell layer nor the capillary network of the lamina propria commonly seen in normal urothelium were visualized with pCLE of urothelial carcinoma, including Ta, T1, and CIS.

Among the most challenging lesions to diagnose on WLC, CIS appears typically as erythematous patches, which are difficult to differentiate from benign conditions, such as post-BCG granulomatous reaction, Foley catheter reaction, urinary tract infections, or scarring from previous resection. In our study, 7 of the high-grade tumors imaged were confirmed to be CIS. Figure 4 shows a comparison between CIS and benign conditions. Confocal features of CIS include larger, more pleomorphic cells compared to inflammatory conditions, indistinct cell borders, and extensive acellular areas that may be due to denuded urothelium. In contrast, confocal imaging of tissue with inflammation showed loosely arranged aggregations of smaller monomorphic cells in the lamina propria consistent with local recruitment of inflammatory cells. Confocal images of scar tissue revealed characteristics similar to the intermediate cells and lamina propria of normal urothelium.

DISCUSSION

In this study, we have compiled a confocal imaging atlas of the lower and upper urinary tract and developed diagnostic criteria for normal, inflammatory, and malignant lesions of the bladder. Expanding on our feasibility report (n = 27),[8] we have confirmed the safety profile of fluorescein administration. Key criteria for normal and benign epithelium include uniform cellular architecture, and visualization of the lamina propria layer and its capillary network. Low-grade carcinoma was characterized by fibrovascular stalks, and high cellular density, whereas high-grade carcinoma was characterized by irregular architecture and pleomorphic cells. These distinct characteristics were consistently observed in normal urothelium and bladder cancer. Development of objective diagnostic criteria is essential for future studies on the diagnostic accuracy (sensitivity, specificity, and positive and negative predictive value) of pCLE in the urinary tract.

Previously, we had found the small FOV and motion sensitivity of the confocal probe to be limitations.[8] In the present study, the mosaicing algorithm was used during offline analysis of confocal video sequences to create static images with wider FOV and to compensate for motion introduced by the operator or the subject (eg, diaphragmatic motion or vascular pulsation). For example, mosaicing of the prostatic urethra images enabled us to visualize a single prostatic gland within the context of other glands in the stroma (Fig. 1B). If applied in real time during TURBT, this mosaicing algorithm may potentially delineate tumor boundaries by highlighting the transitional area of the lesion with adjacent normal tissue, especially in the case of broad based tumors or CIS where the borders are not distinct on WLC.

Another previously reported limitation of pCLE is the lack of deflectability with the rigid cystoscope, resulting in difficulty establishing perpendicular contact of the confocal probe with the mucosa in certain parts of the bladder (eg, anterior).[8] We have investigated the use of a 1.4-mm probe that fits inside the flexible cystoscope and report the in-depth comparative analysis of the 2.6- and 1.4-mm probes elsewhere.[22] Our preliminary ex vivo

experience of applying pCLE to the upper urinary tract was favorable (Fig. 2). With the availability of confocal probes less than 1 mm in diameter,[23,24] in vivo application of pCLE for upper tract pathology will be investigated in the future. The possibility of in vivo optical biopsy of the upper urinary tract with pCLE is particularly attractive, given the challenges associated with obtaining physical biopsies of high quality through standard ureteroscopes.

Our study has limitations, including observer bias inherent in our single center experience. Image analysis was performed retrospectively after pathologic confirmation using H&E, which may have biased chosen confocal characteristics. As with all new technologies, there is an associated learning curve, in part based on the different plane of examination with the respective technologies. Because confocal microscopy emphasizes the cells within the superficial layer of the mucosa, the interpreter must consider cell size and planar cellular organization (or disorganization) over the traditional histopathologic features of cellular stratification and nuclear size and pleomorphism. In our ongoing diagnostic accuracy study, confocal images will be reviewed offline and characterized with these diagnostic criteria by multiple blinded reviewers to assess interobserver variability and reduce diagnostic bias from WLC and pathologic findings.

Images in this study were obtained after fluorescein administration intravesically, intravenously, or both. Although the intravenous route offers greater efficiency (ie, image acquisition can start within 1–2 minutes of administration) and subjectively more consistent staining, efflux of fluorescent urine from the ureteral orifices occurs as short as 3–5 minutes after intravenous administration, which may potentially impair visualization during TURBT. Due to this concern, intravesical administration has become our route of choice for bladder imaging. Intravenous fluorescein can still be administered after intravesical administration, if topical staining was suboptimal and extravesical imaging (eg, prostate, urethra) is desired. Interestingly, we have found that similar to indigo carmine, intravenous fluorescein may be used to identify ureteral orifices intraoperatively.

pCLE is inherently limited by reliance on macroscopic optical imaging (WLC in our study) to identify regions of interest for further microscopic characterization, as it is not practical to survey the entire bladder with pCLE. Combining pCLE with other macroscopic, “red flag” technologies, such as fluorescence cystoscopy or narrow band imaging may be useful to better characterize flat lesions, such as CIS, which remain the most significant challenge across all technology platforms. Nuclear morphology, which is critical for standard tumor grading based on H&E, is not possible since fluorescein only stains extracellularly.

A promising approach to identify neoplastic lesions endoscopically with molecular specificity is the use of fluorescently labeled cancer-specific peptides in conjunction with pCLE.[25,26] With the well-established track record of intravesical therapy, the bladder provides an attractive route to investigate the feasibility of endoscopic molecular imaging.

CONCLUSIONS

We have compiled representative confocal images from the entire urinary tract, including the first imaging of the upper tract, into a confocal imaging atlas. We propose these confocal

diagnostic imaging criteria for normal, inflammatory, and low and high grade cancer to enable adaptation of pCLE as an adjunctive imaging modality for bladder cancer. Current prospective diagnostic accuracy studies are underway to assess the sensitivity and specificity of these confocal criteria in the diagnosis of bladder cancer.

Acknowledgments

We thank Stanford University Cancer Center Developmental Cancer Research Award (to J.C.L.) for funding and Mauna Kea Technologies for technical support. Assistance from the VAPAHCS operating room staff is gratefully acknowledged.

References

1. Lee CS, Yoon CY, Witjes JA. The past, present and future of cystoscopy: the fusion of cystoscopy and novel imaging technology. BJU Int. 2008; 102:1228–1233. [PubMed: 19035886]
2. Cauberg EC, de Bruin DM, Faber DJ, et al. A new generation of optical diagnostics for bladder cancer: technology, diagnostic accuracy, and future applications. Eur Urol. 2009; 56:287–296. [PubMed: 19285787]
3. Cauberg EC, Kloen S, Visser M, et al. Narrow Band Imaging Cystoscopy Improves the Detection of non-muscle-invasive Bladder Cancer. Urology. 2010; 76:658. [PubMed: 20223505]
4. Goh AC, Tresser NJ, Shen SS, et al. Optical coherence tomography as an adjunct to white light cystoscopy for intravesical realtime imaging and staging of bladder cancer. Urology. 2008; 72:133–137. [PubMed: 18598789]
5. Herr H, Donat M, Dalbagni G, et al. Narrow-band imaging cystoscopy to evaluate bladder tumours—individual surgeon variability. BJU Int. 2010; 106:53–55. [PubMed: 20002669]
6. Schmidbauer J, Remzi M, Klatte T, et al. Fluorescence cystoscopy with high-resolution optical coherence tomography imaging as an adjunct reduces false-positive findings in the diagnosis of urothelial carcinoma of the bladder. Eur Urol. 2009; 56:914. [PubMed: 19674831]
7. Witjes JA, Redorta JP, Jacqmin D, et al. Hexaminolevulinate-guided fluorescence cystoscopy in the diagnosis and follow-up of patients with non-muscle-invasive bladder cancer: review of the evidence and recommendations. Eur Urol. 2010; 57:607. [PubMed: 20116164]
8. Sonn GA, Jones SN, Tarin TV, et al. Optical biopsy of human bladder neoplasia with in vivo confocal laser endomicroscopy. J Urol. 2009; 182:1299–1305. [PubMed: 19683270]
9. Sonn GA, Mach KE, Jensen K, et al. Fibered confocal microscopy of bladder tumors: an ex vivo study. J Endourol. 2009; 23:197–201. [PubMed: 19196063]
10. Banno K, Niwa Y, Miyahara R, et al. Confocal endomicroscopy for phenotypic diagnosis of gastric cancer. J Gastroenterol Hepatol. 2010; 25:712–718. [PubMed: 20492327]
11. Dunbar KB, Okolo P 3rd, Montgomery E, et al. Confocal laser endomicroscopy in Barrett's esophagus and endoscopically inapparent Barrett's neoplasia: a prospective, randomized, double-blind, controlled, crossover trial. Gastrointest Endosc. 2009; 70:645–654. [PubMed: 19559419]
12. Thiberville L, Moreno-Swirc S, Vercauteren T, et al. In vivo imaging of the bronchial wall microstructure using fibered confocal fluorescence microscopy. Am J Respir Crit Care Med. 2007; 175:22–31. [PubMed: 17023733]
13. Thiberville L, Salaun M, Lachkar S, et al. Human in vivo fluorescence microimaging of the alveolar ducts and sacs during bronchoscopy. Eur Respir J. 2009; 33:974–985. [PubMed: 19213792]
14. Wang TD, Friedland S, Sahbaie P, et al. Functional imaging of colonic mucosa with a fibered confocal microscope for real-time in vivo pathology. Clin Gastroenterol Hepatol. 2007; 5:1300–1305. [PubMed: 17936692]
15. Wallace MB, Sharma P, Lightdale C, et al. Preliminary accuracy and interobserver agreement for the detection of intraepithelial neoplasia in Barrett's esophagus with probe-based confocal laser endomicroscopy. Gastrointest Endosc. 2010; 72:19. [PubMed: 20381042]

16. Becker V, Vercauteren T, von Weyhern CH, et al. High-resolution miniprobe-based confocal microscopy in combination with video mosaicing (with video). Gastrointest Endosc. 2007; 66:1001–1007. [PubMed: 17767932]

17. De Palma GD, Staibano S, Siciliano S, et al. In vivo characterisation of superficial colorectal neoplastic lesions with high-resolution probe-based confocal laser endomicroscopy in combination with video-mosaicing: a feasibility study to enhance routine endoscopy. Dig Liver Dis. 2010; 42(11):791–797. [PubMed: 20409761]

18. Vercauteren T, Perchant A, Malandain G, et al. Robust mosaicing with correction of motion distortions and tissue deformations for in vivo fibered microscopy. Med Image Anal. 2006; 10:673–692. [PubMed: 16887375]

19. Wallace MB, Meining A, Canto MI, et al. The safety of intravenous fluorescein for confocal laser endomicroscopy in the gastrointestinal tract. Aliment Pharmacol Ther. 2010; 31:548–552. [PubMed: 20002025]

20. Rickard A, Dorokhov N, Ryerse J, et al. Characterization of tight junction proteins in cultured human urothelial cells. In Vitro Cell Dev Biol Anim. 2008; 44:261–267. [PubMed: 18553212]

21. Yu W, Khandelwal P, Apodaca G. Distinct apical and basolateral membrane requirements for stretch-induced membrane traffic at the apical surface of bladder umbrella cells. Mol Biol Cell. 2009; 20:282–295. [PubMed: 18987341]

22. Adams W, Wu K, Liu J-J, Hsiao ST, Jensen KC, Liao JC. Comparison of 2.6 mm and 1.4 mm imaging probes for confocal laser endomicroscopy of the urinary tract. J Endourol. 2011 In Press.

23. Becker V, Wallace MB, Fockens P, et al. Needle-based confocal endomicroscopy for in vivo histology of intra-abdominal organs: first results in a porcine model (with video). Gastrointest Endosc. 2010; 71(7):1260–1266. [PubMed: 20421104]

24. Meining A. Confocal endomicroscopy. Gastrointest Endosc Clin N Am. 2009; 19:629–635. [PubMed: 19917468]

25. Hsiung PL, Hardy J, Friedland S, et al. Detection of colonic dysplasia in vivo using a targeted heptapeptide and confocal microendoscopy. Nat Med. 2008; 14:454–458. [PubMed: 18345013]

26. Li M, Anastassiades CP, Joshi B, et al. Affinity peptide for targeted detection of dysplasia in Barrett's esophagus. Gastroenterology. 2010; 139(5):1472–1480. [PubMed: 20637198]

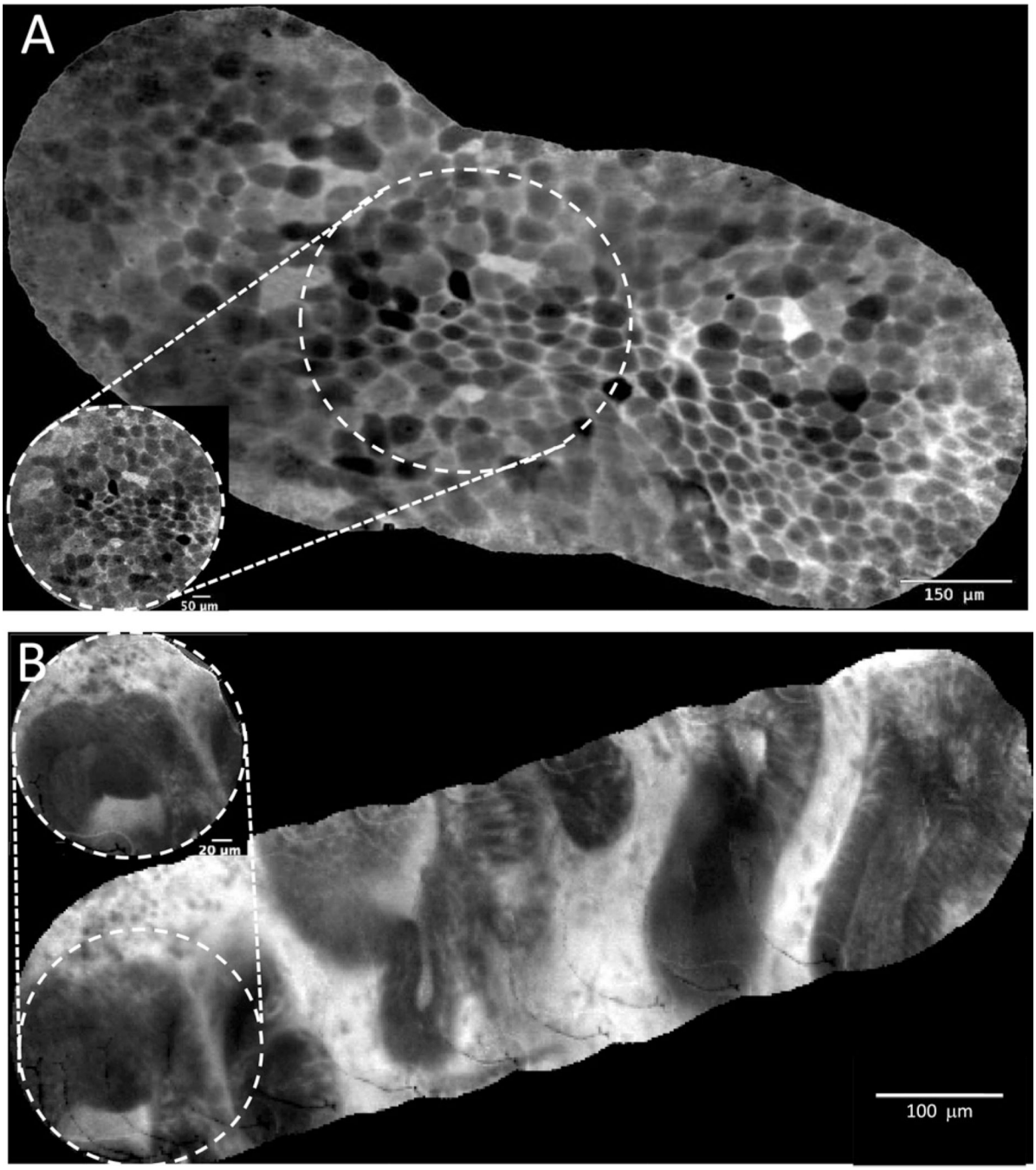

Figure 1.

Confocal image processing with *mosaicing* algorithm that generates panoramic view of the tissue microarchitecture with improved clarity compared to single image frames (inset). (**A**) Normal bladder urothelium showing umbrella cell layer: note the characteristic large polygonal-shaped cells. (**B**) Normal prostate imaged through prostatic urethra with multiple dark prostate glands within the white stroma. Note the mosaics significantly increased the overall field of view by ~5-fold.

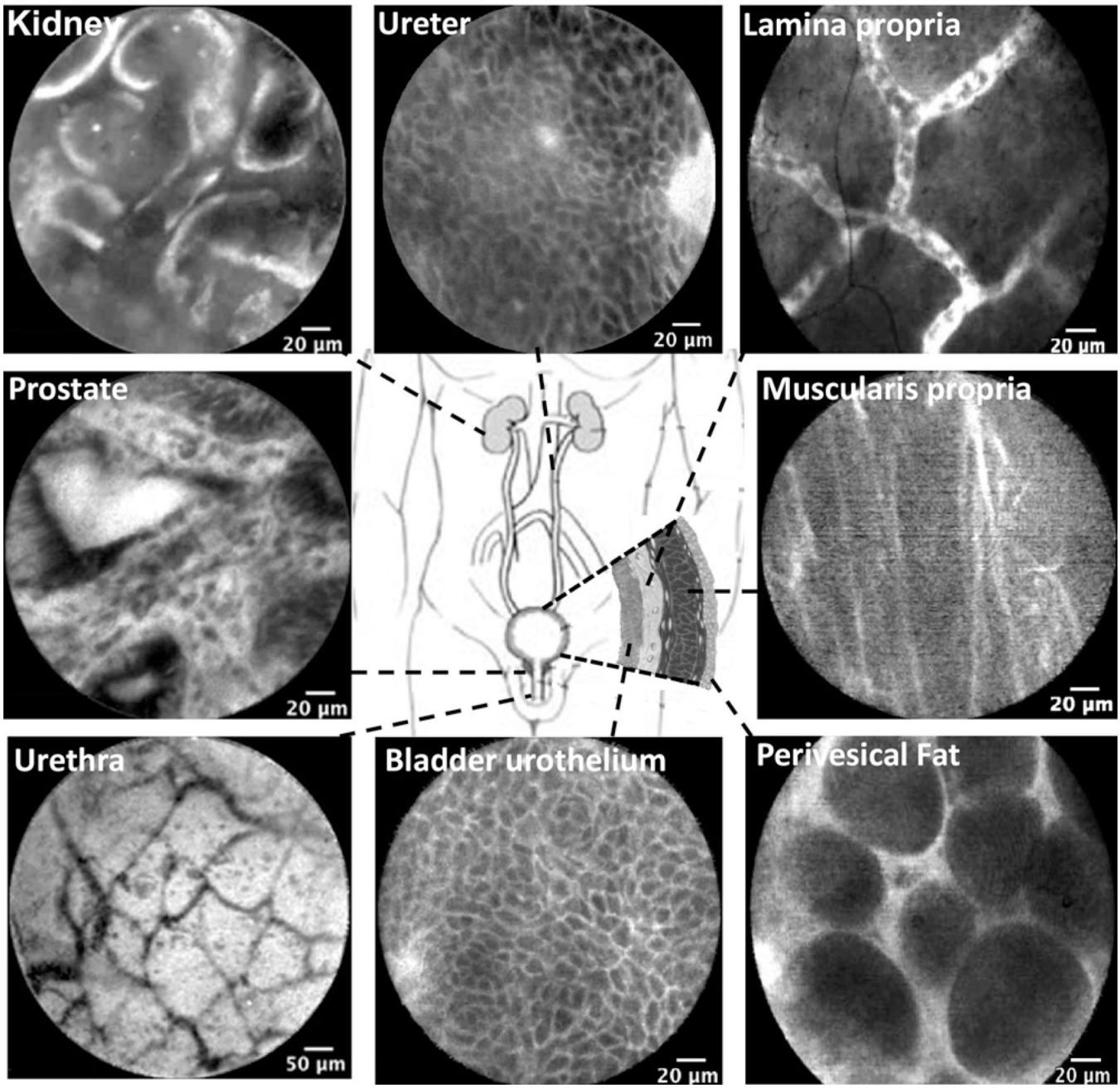

Figure 2.

Probe-based confocal laser endomicroscopy (pCLE) images of the normal urinary tract. All images of the lower urinary tract were acquired in vivo, whereas upper tract images (kidney cortex and ureter) were acquired ex vivo. Note similarities of the urothelium (intermediate cells) between ureter and bladder. Lamina propria is characterized by capillary network of moving erythrocytes. Muscularis propia and perivesical fat images were obtained from the tumor resection bed.

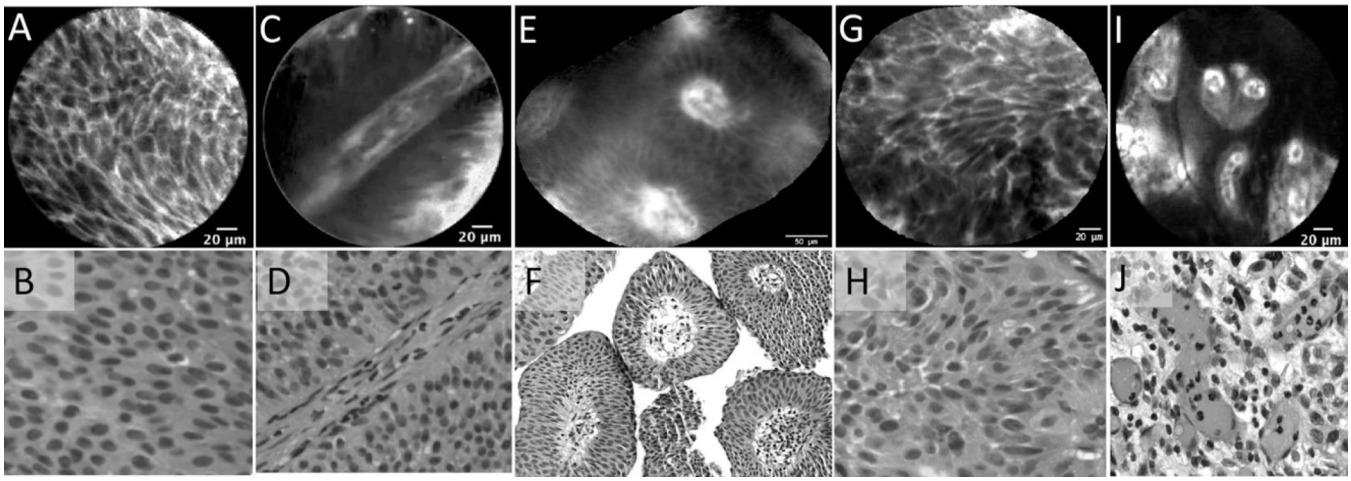

Figure 3.

Characteristic in vivo microscopy features of low and high grade urothelial carcinoma compared with corresponding H&E sections. Low grade urothelial carcinoma: (**A, B**) Crowding of uniform-appearing cells. (**C, D**) Fibrovascular stalk with a thickened endothelial layer. (**E, F**) Cross-sectional mosaic view of the fibrovascular stalk containing erythrocytes in the vascular core. High-grade urothelial carcinoma: (**G, H**) Pleomorphic and distorted sheet of cells. (**I, J**) Distorted fibrovascular stalk with variably sized vascular cores.

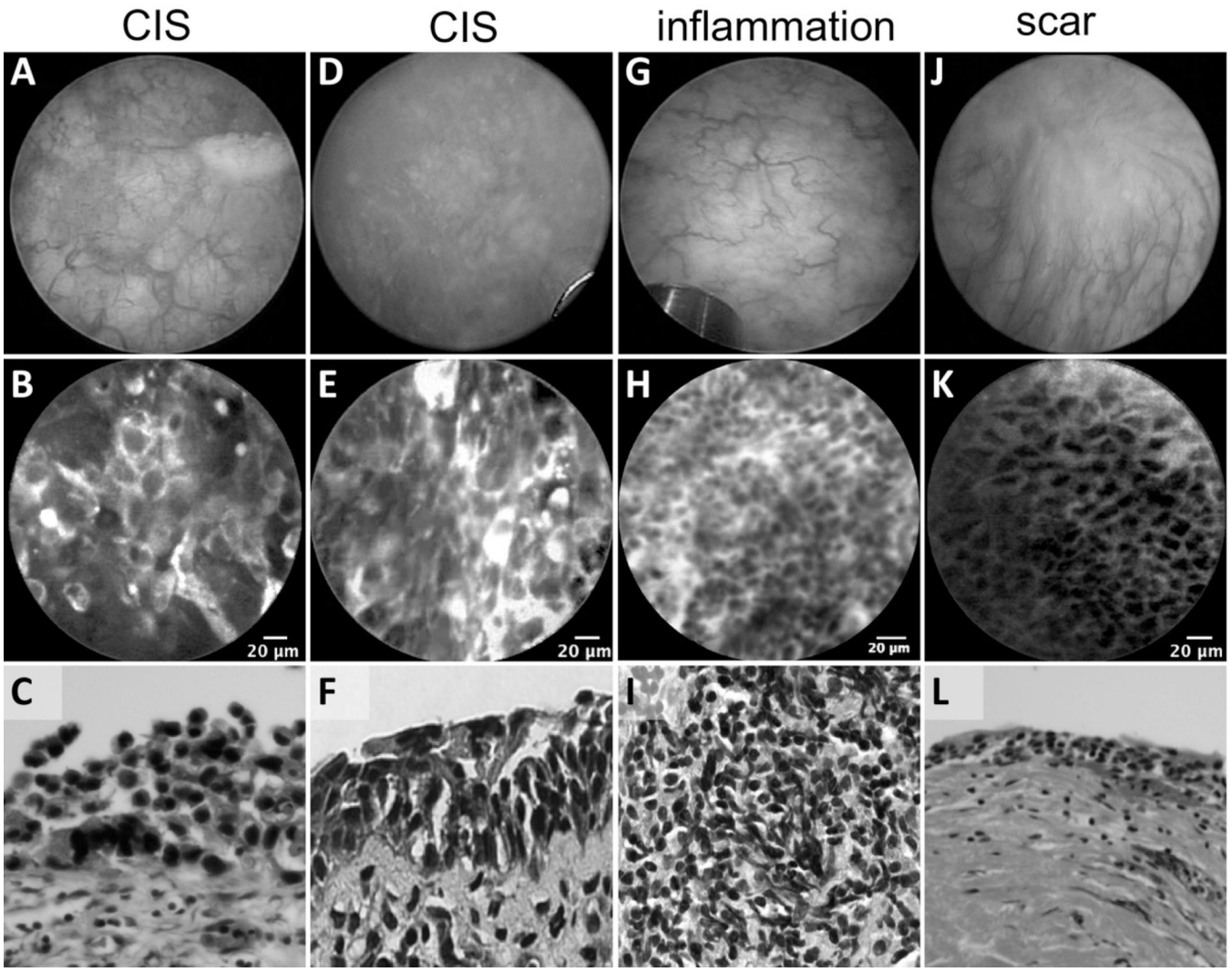

Figure 4.

Images of erythematous flat lesions in the bladder by WLC, pCLE, and corresponding H&E sections. (**A and D**) Cystoscopic view of erythematous patches in 2 patients with CIS. Cautery mark in A used to coregister pCLE imaging and biopsy site. (**B and E**) Confocal images showing large pleomorphic cells, loss of cellular cohesiveness, and indistinct cellular borders. (**C and F**) Characteristic histologic images of CIS, with full-thickness high-grade cellular atypia, increased nuclear/cytoplasmic ratios, nuclear hyperchromasia, nuclear pleomorphism, and cellular discohesion. (**G**) Erythematous patch on WLC with (**H**) small monomorphic cells infiltrating the lamina propria and (**I**) chronic lymphocytic infiltrate on histology. (**J**) Patient with scar from previous TURBT showing (**K**) normal appearing intermediate cells with clear cell borders and (**L**) thickened lamina propria on histology.